

## AN INVESTIGATION INTO PARAMETRIC EFFECTS ON BOILING HEAT TRANSFER

Mehmet Arik  
Ozyegin University  
Department of Mechanical Engineering  
Cekmekoy, İstanbul, Turkey  
E-mail: [mehmet.arik@ozyegin.edu.tr](mailto:mehmet.arik@ozyegin.edu.tr)

### ABSTRACT

With the advanced electronics systems, heat fluxes are also elevated over  $100 \text{ W/cm}^2$  at local hot spots. Therefore, to meet this aggressive thermal need both academia and industry have studied liquid cooling with dielectric fluids especially with perfluorocarbons. Elevated pressures, dielectric fluids mixtures, subcooling, and surface enhancement techniques have been studied to enhance the peak heat flux in pool boiling called CHF. This paper is going to discuss the experimental results of pool boiling and CHF for various heaters (silicon and Beryllium Oxide). Both subcooling and pressure effects over the boiling curves and CHF values have been investigated. It is found that current heater show a stronger dependence on subcooling for the CHF values. A weaker shift of the boiling curve with the elevated pressure has also been observed.

### INTRODUCTION

Boiling heat transfer is observed in a number of practical applications such as heat exchangers, food industry and water treatment processes. Liquid cooling provides tremendous amount of heat removal capability due to latent heat of evaporation. Evaporation occurs in nucleation sites at a liquid-solid interface and produces bubbles followed by bubble columns and vapor blanket. The rate of heat transfer depends on a number of parameters such as; liquid temperature (subcooling), pressure, liquid properties, heater geometry, heater surface, and heater orientation. In nucleate pool boiling, the heat flux increases steeply with the surface superheat but when the generated vapor bubbles blanket the surface, a large temperature increase on the heater surface results, leading to the Critical Heat Flux (i.e. CHF) condition and the termination of nucleate pool boiling [2]. This condition is also known as the burn out point and the peak or maximum heat flux, and is associated with a rapid temperature rise of 10s or 100s of degrees C.

A large number of studies have focused on predicting the subcooling effect. A pioneering study completed in 1951 by Kutateladze [3] suggested that the CHF in subcooled liquid should increase relative to the saturated pool boiling CHF value and depends on the Jacob number. To confirm this

understanding, Kutateladze and Schneiderman [3] performed subcooling experiments with rod heaters in various liquids (i.e. water, iso-octane, and ethanol). Their reported results showed that CHF increased linearly with increasing subcooling. One of the most widely quoted studies was performed by Ivey and Morris [4]. Their experimental studies were performed in water with wire heaters, and a correlation was proposed linking CHF to the Jacob number.

CHF in dielectric liquids, for possible use in the thermal management of electronic components, has been of interest for the last several decades. Hwang and Moran [5], in one of the early studies, presented experimental results for FC-86 boiling on 4.57 mm square heaters. A subcooling range of 0-80 K was studied on the vertically oriented heaters. An increase in CHF with increasing subcooling was observed. Morozov [6] measured CHF on thin nichrome wire heaters in methyl isopropyl alcohol for pressures ranging from atmospheric to 0.90 of the critical pressure of the liquid. He found that CHF initially increased with increasing pressure and attained a maximum value at approximately 0.35 of the critical pressure before decreasing at higher pressures. Lienhard and Shrock [7] performed studies on pressure effects for wire heaters in water, acetone, benzene, methyl alcohol and isopropyl alcohol environments and observed an increase in CHF values with elevated pressures similar to the previous studies [8]. They reported that the Kutateladze-Zuber correlation was able to account for the pressure effects and successfully predict CHF. Later, the effect of pressure on CHF for FC-72 boiling on square, vertically oriented, copper heaters has been studied by Anderson and Mudawar [10] for a pressure range of 101.3 to 303.9 kPa. A 23% increase in the CHF was observed with an increased pressure from atmospheric conditions to 202.7 kPa, but only an additional 3.7% increase was observed as the pressure was further raised to 303.9 kPa.

Bergles [12] continued to investigate subcooling effects on CHF for FC-72 boiling on a vertically oriented thin nichrome foil heater. The most notable observation was that the rate of CHF increase with subcooling diminished as the pressure increased, due to the effect of pressure on the density ratio. The effect of bulk temperature was also studied by Carvalho and Bergles [14] for boiling in a dielectric liquid, FC-72, from thin,

nichrome foil heaters. To simulate electronic chips, they also performed experiments with silicon chips. At high heat fluxes, different enhancement techniques produced approximately the same wall superheat. Brusstar and Merte [14] studied effects of heater surface orientation and subcooling on the CHF. They presented a model for low velocity flow and pool boiling. They modeled the effect of subcooling such that the volume of vapor produced at CHF was independent of subcooling for a given orientation.

Some of the pool boiling experiments performed by Lee et al. [17] included the results of subcooled pool boiling of FC-84 and FC-104 for both pure liquids and binary mixtures with flat heaters. Subcooling was as high as 50 K, and a similar behavior to the previous studies was reported. Watwe [20] performed a series of experiments using a plastic pin grid array silicon heater (i.e. PPGA) immersed in FC-72, and observed similar effects of pressure on the pool boiling CHF. Watwe et al [20] presented experimental results of FC-72 with PPGA chip package for a wide range of subcooling; spanning the range of the 0-70 K.

Kandlikar [22] performed a study for CHF in subcooled flow boiling. In addition to his own experimental results, more data were collected to evaluate subcooling effects in both flow and pool boiling. His results displayed a similar trend (linear increase with decreasing bulk temperature) to that reported in the literature. In the experimental study of Arik [23] a linear increase of heat flux with elevated subcooling at atmospheric pressure was observed using FC-72 as the working fluid. The author repeated the experiments at elevated pressure and found that the subcooling enhancements were interestingly very similar to the atmospheric pressure conditions. The increased pressure did not diminish the subcooling effect.

Rainey et al. [24] investigated the effect of subcooling on CHF from 1cm<sup>2</sup> flat and micro porous enhanced surfaces in FC-72. They operated over a broad liquid subcooling range (0-50K). The subcooling delayed the formation of the dry out condition and thus increased CHF. They also recorded an increase in CHF with micro porous surfaces. Moreover, they found that the enhancement of CHF due to the increase in

subcooling was greater for micro porous surfaces, consisting of aluminum particles (1 to 20 μm in diameter) and a binder with thickness of approximately 50 μm, than for plain surfaces. El-Genk and Parker [26] investigated pool boiling of saturated and subcooled HFE-7100 from both plain copper and porous graphite surfaces measuring 10 mm x10 mm. They detected an increase in CHF with subcooling for both types of test surfaces. A broad literature survey to enhance pool boiling CHF was presented by Arik et al [27]. They presented passive pool boiling with dielectric fluids, including the effects of subcooling, pressure, length scale, mixtures, surface enhancements, and nano-additives, has been presented collected from a large number of studied. It is found that CHF can be enhanced over 100 W/cm<sup>2</sup> by the combined effects of subcooling, pressure, surface treatment and mixtures.

The subcooling effect is seen to be very strong at atmospheric pressure and to decrease in impact with an elevation in pressures. It might be expected that for a fixed liquid temperature, the increased subcooling accompanying a rise in pressure would lead to higher CHF, while the decrease in latent heat, density ratio, and surface tension encountered at higher pressure would weaken CHF. It appears that the next result – in the range tested for FC-72 – creates a substantial pressure-related enhancement.

The objective of the current study is understanding the effect of subcooling pressure on the CHF for various chip packages including Si and BeO. Therefore, an experimental study has been carried out and results are presented in tabular and graphical forms.

**EXPERIMENTAL STUDY**

Figure 1 shows the test set-up for the CHF experiments manufactured for the current study. Experiments were conducted in a stainless steel test vessel operated up to 500 kPa in pressure. The tank includes two windows for the visual observation of the heat transfer phenomenon from the chip package.

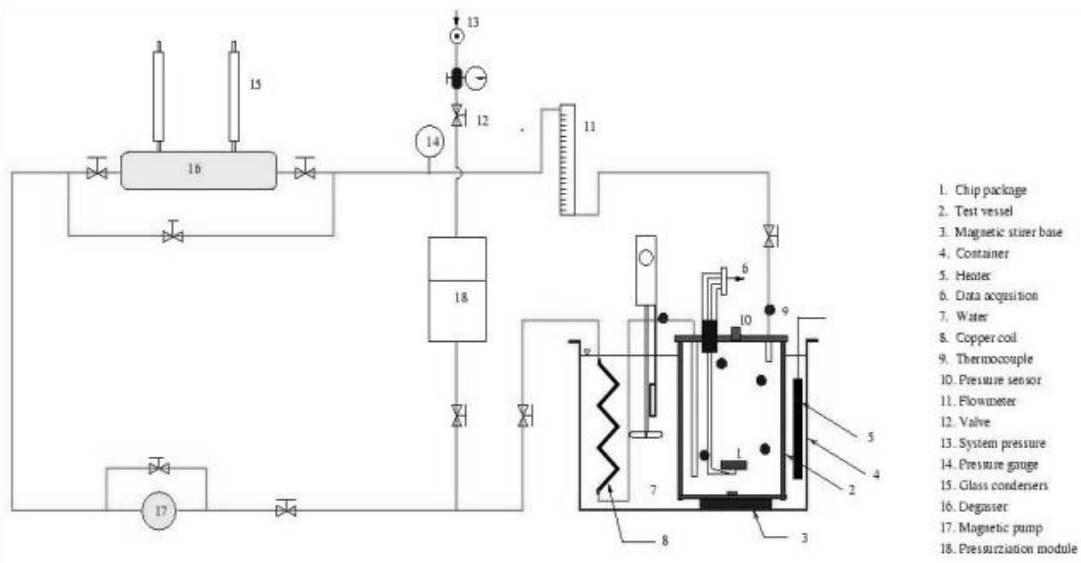


Figure 1: Pool boiling experimental set-up [29]

A Lexan container filled with water is used to control the coolant temperature in the vessel. To condition the test fluid (FC-72), coolant passed through a copper coil, which is immersed in the water. A piezo-resistive pressure transducer is placed on the cover of the test vessel to measure the pressure in

the tank. A precision resistor is used to accurately measure the current flowing in the power line. Temperature measurements were performed with diodes and thermocouples. The fluid temperature was measured by using T-type thermocouples. Further details of this apparatus may be found in Arik [29].

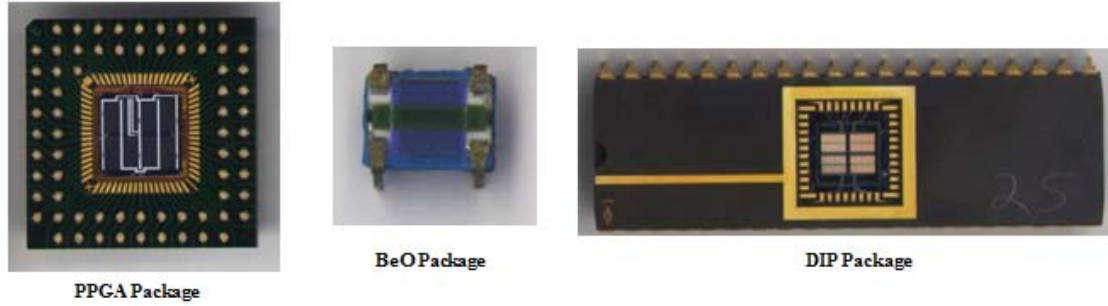


Figure 2: Dual Inline Package (i.e. DIP) with smooth Silicon surface (Arik, 2001)

**Test packages:** To enable the direct application of these results to the cooling of electronic components, most of the tests were performed with the DIP chip packages, shown in Figure 2, obtained from Sandia National Laboratories. The package had 20 pins, which provided electrical inputs as well as input/output signals to/from diodes. Six diodes were evenly placed and distributed on the silicon chip and embedded 5  $\mu\text{m}$  under the heater surface. DIP packages have 40 pins for the electrical connections and diode input/outputs. A silicon die (6.5x6.5 mm) was embedded in the package cavity and attached to the package by means of a low conductivity epoxy. The chip carries two heater structures on 2  $\mu\text{m}$  lines and spacing using poly-silicon conductors oriented perpendicularly to the overlying triple tracks with a nominal resistance of 50 ohms. This package provides five p<sup>+</sup>n diode thermometers, one in the die center and four under the perimeter bond-pads.

**Boiling characteristics in FC-72:** Before we discuss experimental findings, it is worthwhile to take a closer look at some of the fundamental characteristics of the boiling. Bubble departure diameter, bubble departure frequency, and bubble growth and residence time, and thermal penetration depth were calculated in order to assure the correct waiting period before each readings. Rohsenow [30] proposed the following relationship to calculate bubble diameter;

$$D_{\text{bubble}} = \sqrt{\frac{\sigma_f 4.65 \times 10^{-4} \text{Ja}_*^{5/4}}{g(\rho_f - \rho_v)}} \quad (2)$$

Calculated values for the bubble diameters are 0.25 mm, 0.19 mm, and 0.16 mm for the pressures of 101.3 kPa, 202.6 kPa, and 303.9 kPa respectively. Malenkov (1968) proposed the following correlation to calculate the bubble departure frequency;

$$f = \frac{U_b}{D_b \left[ \pi \left( 1 - \frac{1}{1 + U_b \rho_v h_{fg} / q} \right) \right]} \quad (3)$$

where 
$$U_b = \left[ \frac{g D_b (\rho_f - \rho_v)}{2(\rho_f + \rho_v)} + \frac{2\sigma_f}{D_b(\rho_f + \rho_v)} \right]^{0.5}$$

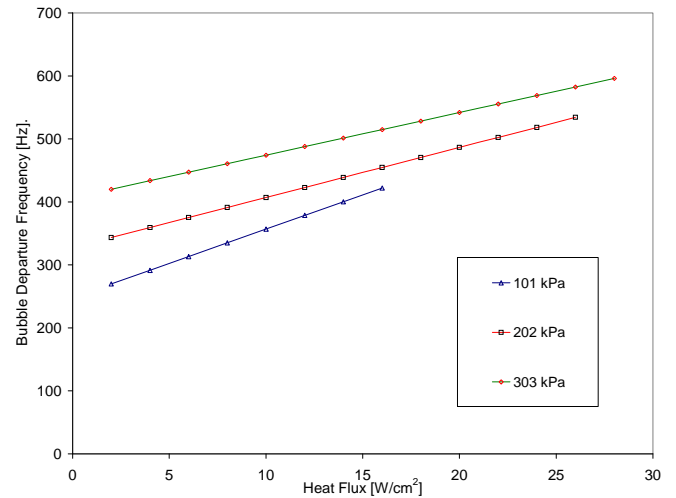


Figure 3: Variation of the bubble departure frequency with the heat flux.

Figure 3 presents the bubble departure frequency with the corresponding heat flux. It may be seen that lower pressure values create lower departure frequency and that the frequency increased when the heat flux increased. Moreover, the slope of the curve diminishes with the increasing pressures. This behavior was also observed visually during these experiments. Higher bulk temperature, and hence low subcooling, produced very strong liquid columns as a result of high bubble departure frequencies. Hovering period usually used for the bubble mushroom consists of the bubble waiting time and growth time

and they are often assumed to be equal. The bubble departure frequency is given as;

$$f = \frac{1}{\tau} \quad (4)$$

Figure 4 presents the variation of the bubble with heat flux for a range of pressures. Since the bubble departure frequency and the hovering period are inversely proportional, large waiting periods are obtained for low pressures. At atmospheric pressure, when the package experienced a heat flux of 12 W/cm<sup>2</sup>, the bubble period was found to be 2.8 milliseconds. Since the waiting period in the data acquisition program set to 120 seconds so that it will give enough time to the liquid on the heater surface in order to fully evaporate. For the same heat flux rate at P=303.9 kPa, the hovering period was about 2.1 milliseconds. Then, the hovering period does decrease with the elevated pressures.

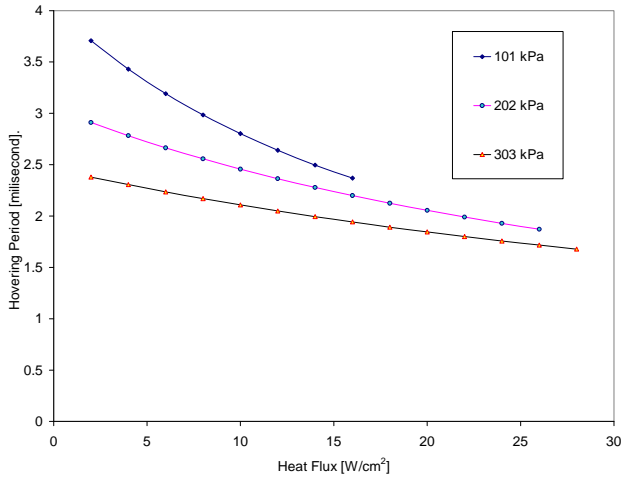


Figure 4: Variation of the bubble period with the heat flux. The superheated layer thickness along the wall is calculated by means of transient conduction heat transfer. The thermal penetration depth can be given as in Incropera and DeWitt [31];

$$\delta_{\text{liquid}} = \sqrt{12\alpha\tau_w} \quad (5)$$

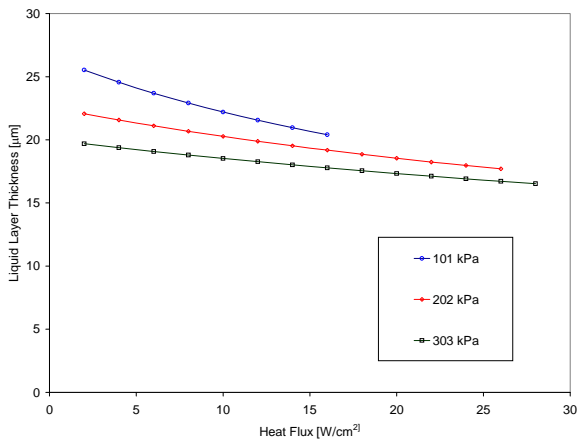


Figure 5: Variation of the superheat liquid layer thickness with the chip flux.

Figure 5 presents the variation of the superheated layer thickness with the chip heat flux. The liquid thickness showed a similar behavior to the bubble period. The higher the pressure, the thinner the layer thickness. At the standard pressure and  $q''=12.5 \text{ W/cm}^2$ , the predicted liquid thickness was found to be 23.4 μm., although at high pressures (303.9 kPa), it decreased to 75 percent of standard pressure condition. Arik and Bar-Cohen presented a CHF correlation [25]. This correlation for pool boiling CHF, which was derived for horizontal, square heaters, is shown in equation (1);

$$q''_{\text{CHF, TME}} = \frac{\pi}{24} h_{\text{fv}} \sqrt{\rho_v} [\sigma_f g (\rho_f - \rho_v)]^{1/4} \left( \frac{S}{S+0.1} \right) [1 + < 0.3014 - 0.01507L'(P) >] (1 + 0.030 \left[ \left( \frac{\rho_f}{\rho_v} \right)^{0.75} \frac{c_{p_f}}{h_{\text{fv}}} \Delta T_{\text{sub}} \right]) \quad (6)$$

where  $L'(P) = L \sqrt{\frac{g(\rho_f - \rho_v)}{\sigma}}$

The first term on the right side represents the classical Kutateladze-Zuber prediction, considered the upper limit, saturation value of CHF on very large horizontal heaters. The second term is the effect of heater thickness and thermal properties. The third term accounts for the influence of the length scale on the CHF and is equal to unity or higher. The last term represents the influence of subcooling on CHF.

## RESULTS AND DISCUSSIONS

A number of experiments have been performed a part of this study. Three different chip packages have been used. Two of them had Silicon surfaces (PPGA, DIP), while the other one had Beryllium Oxide. Experimental findings for all those packages will be presented in the subsequent sections. First, a series of experiments with Motorola PPGA packages were performed for a range of sub cooling conditions with gassy FC-72 at atmospheric conditions to determine the effect of the sub cooling on CHF. Results are presented in Table 1. Heat flux increments were chosen as 0.25 W/cm<sup>2</sup> during the experiments to capture CHF accurately.

Table 1: Results and comparison of CHF experiments with DIP and PPGA packages at P=1 Bar.

$\Delta T_{\text{sub}}$ [K]	CHF <sub>exp</sub> [W/cm <sup>2</sup> ]	CHF <sub>pre</sub> [Eq. 6] [W/cm <sup>2</sup> ]	CHF [PPGA] [W/cm <sup>2</sup> ]
0	17	14.6	18
10	19	16.7	22
30	25	20.9	26
35	30	21.9	28

Satisfactory agreements (i.e. ± 10%) was obtained between the new experiments and published results (Watwe [18]). The correlation was able to predict CHF with high accuracies for

low subcooling although the error band increased for higher subcooling rates. A second series of experiments was performed to continue the CHF research, by using Beryllium Oxide heater packages. Those heaters were 6 mm by 9 mm in rectangular shape with a 0.5 mm thick substrate. Beryllium Oxide heaters were insulated with low conductivity glass material.

Table 2 shows the experimental results obtained with the Beryllium Oxide chip heaters. Both horizontal and vertical heaters have been studied and they are compared with TME CHF correlation (Eq. 6) and published data with silicon surfaces. Experiments for both orientations showed very good agreement with the previous findings. However, the further use of these packages was avoided because of the electrical uncertainties of the package. After exposure to CHF, the electrical behavior of the BeO package has changed so R-T curve was no longer valid. Then, a more reliable, Sandia DIP chip packages (i.e. ATC2.6) were used to collect data during the rest of these research efforts.

Table 2: Experimental and analytical studies with Beryllium Oxide heaters.

$T_{bulk}$ [°C]	P [Bar]	$CHF_{exp}$ [W/cm <sup>2</sup> ]	$CHF_{pre}$ [W/cm <sup>2</sup> ]	CHF (PPGA) [W/cm <sup>2</sup> ]
55	2	20.7	22.7	24.4
20	3	36.4	35.2	34.9
20	1	26.4	23.7	27
55	1	14	15.9	13.5
40	1	18	20.1	17.5

**Boiling curves:** The boiling curves for three different pressures and various bulk temperatures are presented in Figure 6 through Figure 8. Each experiment was repeated at least twice. If there was a difference between the CHF values of less than 3%, no additional experiments were performed. Otherwise, additional experiments were conducted to decrease the uncertainty in the CHF values.

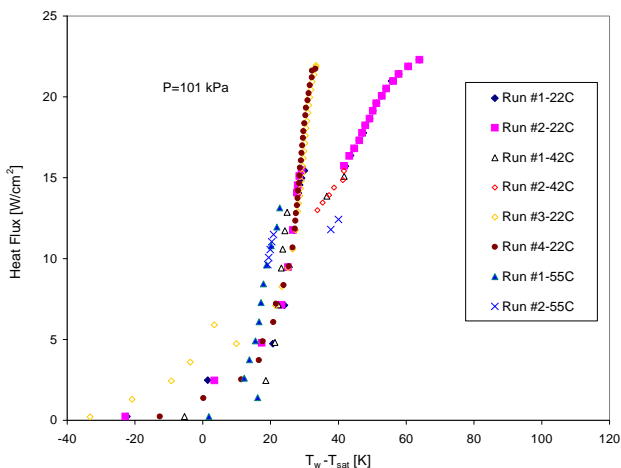


Figure 6: Boiling curves for gassy FC-72 at P=101.3 kPa.

The boiling curves at the standard pressure, for three different bulk temperatures, is given in Figure 6. The

experiment at 22 °C bulk temperature was repeated four times. A good repeatable behavior of the boiling curve can be observed. During the first two runs at 15 W/cm<sup>2</sup>, a temperature jump of 13 K was observed. Since the criteria for CHF was set at a 20 K increase of the package temperature the boiling experiment was allowed to continue. Before and after this sudden temperature increase, a typical temperature increase of 0.2-1 K was noticed during the fully developed nucleate boiling curve. The CHF wall superheat at the standard pressure was as high as 63 K, with the corresponding chip temperature of 119.6 °C. The lowest and the highest CHF values after four runs were found to be 21.8 and 22.3 W/cm<sup>2</sup>. That produces a very small scattering of the heat flux findings.

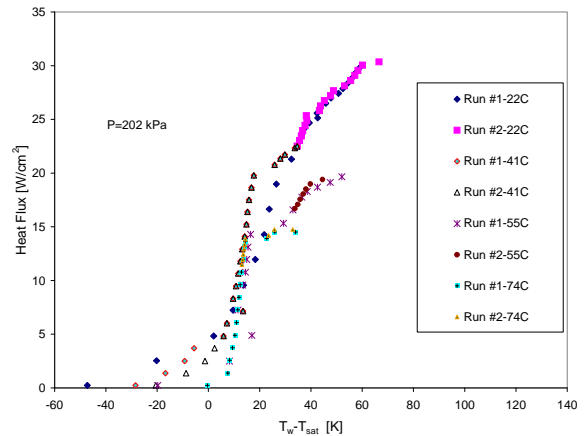


Figure 7: Boiling curves for gassy FC-72 at P=202.6 kPa.

A lower CHF, for the elevated bulk temperature resulting in a lower subcooling, was observed at 41 °C. A temperature jump of 12 degree at the 13.9 W/cm<sup>2</sup> was observed. However, immediately after this jump CHF occurred at 15.1 and 15.4 W/cm<sup>2</sup> during the two consecutive runs. The wall superheat was as high as 41.7 K corresponding to 98.3 °C of the surface temperature. The final experiment at 101.3 kPa was performed at a temperature very close to the saturation temperature of FC-72. This leads to the lowest CHF values, as expected. Although the temperature jump was not observed during the first run, the second run experienced a temperature jump of 15 K and the wall superheat values are 23 K and 40 K respectively.

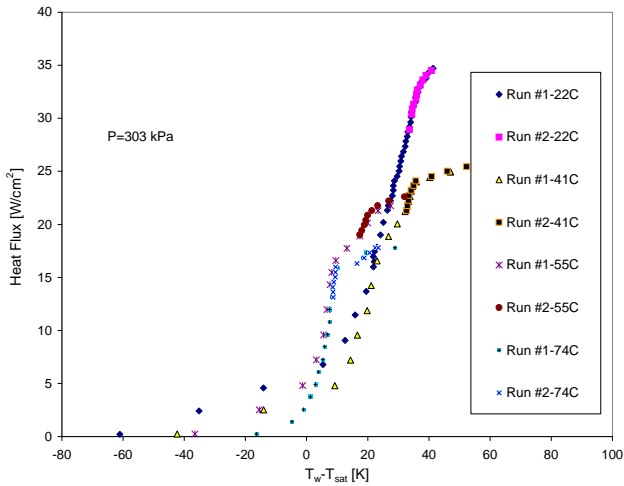


Figure 8: Boiling curves for gassy FC-72 at P=303.9 kPa.

Figure 7 and Figure 8 shows the boiling curves for 202.3 kPa and 303.9 kPa. Higher CHF values were observed with the increasing pressure. A sudden temperature jump, at intermediate heat fluxes, was observed during some of the experiments. However, some of them presented a more stable boiling curve without shifts. These points are not accepted as CHF points because of two reasons. First, the temperature jump was less than 20 K. Secondly, when CHF occurs heat flux was not able to increase. Either a lower heat flux or the flux removed during the last power increment should be observed. However, at these points, the chip was able to remove heat and the jump was not as high as expected. Intermediate pressure experiments, 202.6 kPa, and showed lower wall superheat values than the standard pressures before the boiling jump point. However, at the end of boiling curves wall superheat values were found to be similar.

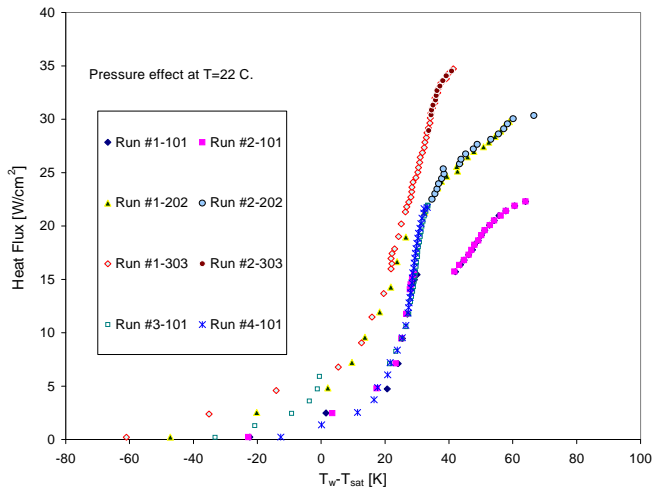


Figure 9: Pressure effects at T<sub>bulk</sub>=21 °C.

Figure 8 presents the boiling curve for the highest pressure. Lower wall superheats were observed until a point, however when the steepness of the slope diminishes, the package experienced high surface temperatures leading to high wall

superheats. At the bulk temperature of 41 °C, the package had a surface temperature of 149.5 °C corresponding to a 56 K wall superheat.

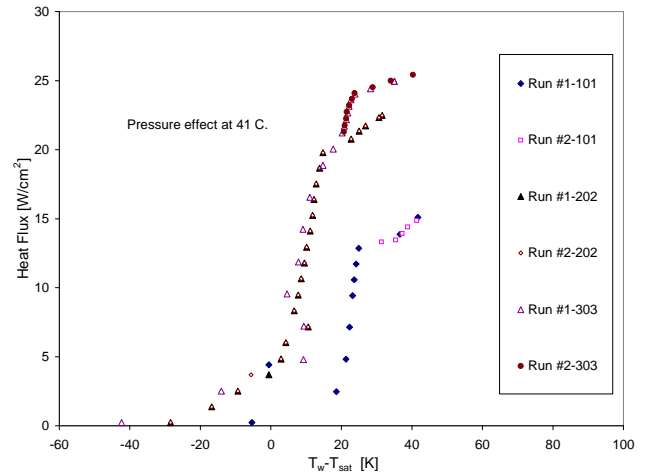


Figure 10: Pressure effects at T<sub>bulk</sub>=41 °C.

**Pressure effects:** Figure 11 through Figure 13 presents the effect of pressure on the CHF with the excellent repeatability of the boiling curves. The experimental findings at the lowest bulk temperature are given in Fig. 4.9. The anticipated shift of the boiling curve towards the left was observed with the increasing pressure.

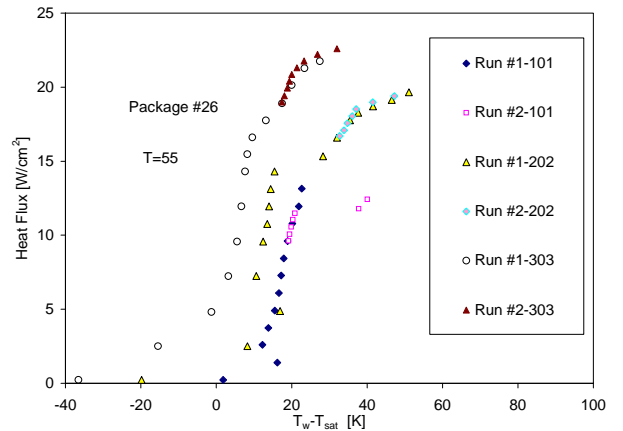


Figure 11: Pressure effects at T<sub>bulk</sub>=55 °C.

A stronger shift resulting in lower wall superheat values can also be seen in Figure 8 and Figure 11 for higher pressures. Although higher CHF values and somewhat lower wall superheat were obtained at 303.9 kPa, the chip surface temperature was not lower than that attained at atmospheric pressure conditions. Since the saturation temperature of FC-72 at 1 atm is given as 56.6 °C [1], the corresponding chip temperature is ~100 °C. However, the chip temperature was found to be 133.5 °C for 3 atm.

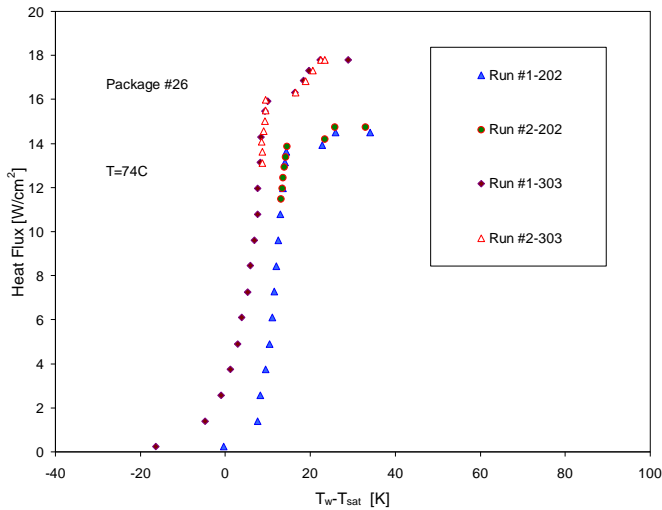


Figure 12: Pressure effects at Tbulk=74 °C.

Previous studies, by Anderson and Mudawar [10] reported that there is little enhancement of CHF after 202.6 kPa. They reported an increase of 3 percent. However, current experimental findings reveal a substantial increase in CHF with the elevated pressure. Figure 13 presents the linear increase of CHF with the pressure. The graph also includes the curve fitting results for three bulk temperatures. The lowest liquid temperature created the steepest slope with a coefficient of 0.0609, decreasing to 0.0 and 0.0460, with increasing temperature. When the bulk temperature was 41 °C, the coefficient was found to be 0.0493. This corresponds to a 21% decrease over the standard conditions. The curve fitting produced a coefficient of 0.0460 for 303.9 kPa that is 24% lower than 101.3 kPa. Therefore, the subcooling is very strong at the standard pressure and it has a decreasing behavior with the elevated pressures. CHF was expected to have an asymptotic increasing behavior until 500 kPa.

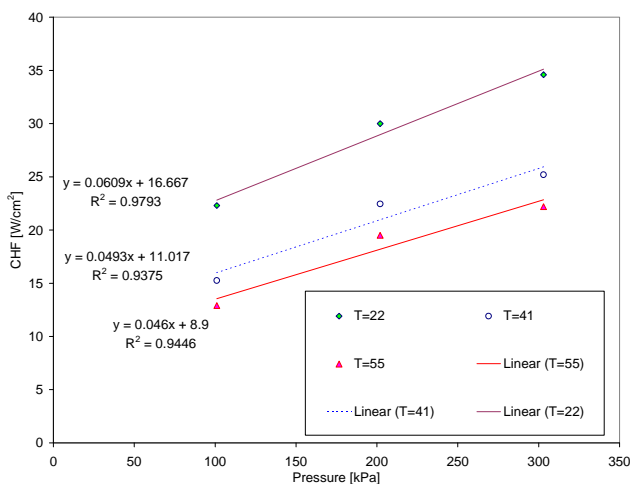


Figure 13: Pressure effect for various liquid temperatures.

**Subcooling effects:** Figure 14 presents the linear increase of heat flux with elevated subcooling at several pressures. Curve fitting was also performed with a linear least square fit to obtain the slope of the curve. The slope of the linear curve was found to be between 0.29 and 0.316 that is very close to the coefficient given in TME correlation. The increased pressure did not diminish the subcooling effect.

The subcooling enhancement for the horizontal DIP packages is higher than observed that by Watwe (1996) but similar to the findings by McNeil [13]. The reason for higher subcooling effect can be related to the rapid condensation of the rising bubbles or columns. The size of the heater might also be an important. Another factor might be the effect of the alumina substrate. DIP packages have a higher substrate surface area than PPGA packages.

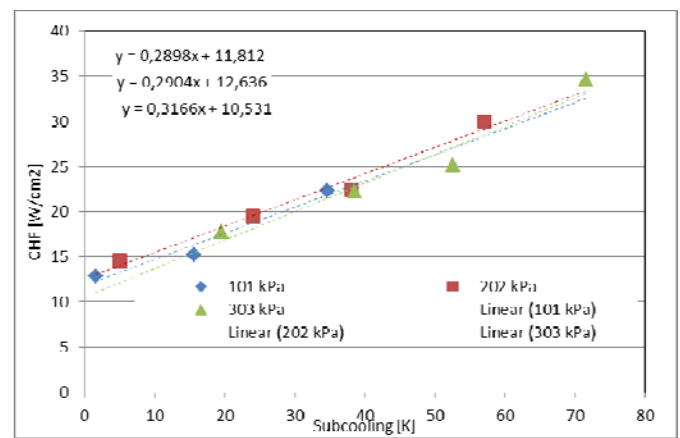


Figure 14: Subcooling effect between 101.3 kPa and 303 kPa.

## CONCLUSIONS

The boiling heat transfer results of experimental findings over chip-like surfaces (Silicon and BeO) have been presented for FC72. Boiling heat transfer to understand subcooling and pressure is presented. Later, a discussion for reaching 150 W/cm<sup>2</sup> has been presented for perfluorocarbons based on the published data by various researchers. Though it quite possible to reach and perhaps exceed 150 W/cm<sup>2</sup>, there are still major obstacles to implement this advanced cooling scheme for practical applications as follows;

- Long term (>10000 hrs) durability of those fluids is not proven in real applications especially for boiling and CHF.
- The effect of CHF on the liquids is not well understood yet and more data needs to be generated.
- Though pressure is a great way of enhancing CHF, it is very hard to implement in real applications
- Surface coating is also another way of advancing CHF beyond current limits, however, nucleate boiling and CHF are very dynamic mechanisms and it may impact long term reliability of the chip.

- The length of the chip can be controlled for some applications; however, the trend is smaller chips and less space.
- Effusivity of the chips can also be controlled but the thinner the chip, the less material it requires.

## NOMENCLATURE

$c_p$	Specific heat [J/kg-K]
$CHF$	Critical heat flux
$C_p$	Specific heat [J/kg-K]
$D$	Bubble diameter [m]
$F$	Frequency [Hz]
$g$	Gravitational acceleration [m/s <sup>2</sup> ]
$h_{fg}$	Latent heat of vaporization [J/kg]
$L$	Length [m]
$m$	Constant
$q$	Heat flux [W/m <sup>2</sup> ]
$P$	Pressure [Pa]
$Pr$	Prandtl number
$S$	Thermal effusivity
$T$	Temperature [°C]
$U$	Velocity [m/s]

## Greek Symbols

$\alpha$	Thermal diffusivity [m <sup>2</sup> /s]
$\mu$	Dynamic viscosity [kg/ms]
$\rho$	Density [kg/m <sup>3</sup> ]
$\sigma$	Surface tension [N/m]
$\Delta T$	Wall superheat [°C]

## Subscripts

$l$	Liquid
$g$	Gas
$s$	surface

## REFERENCES

- 1 3M Specialty Fluids, "[www.3m.com/market/industrial/fluids/library](http://www.3m.com/market/industrial/fluids/library)", 2000.
- 2 M. Arik, A. Kosar, H. Bostancı, A. Bar-Cohen, "Pool Boiling Critical Heat Flux in Dielectric Liquids and Nanofluids", *Advances in Heat Transfer*, Ed. Young Cho and George Greene, Vol. 43, 2011, pp. 1-76.
- 3 Kutateladze, S.S. and Schneiderman, L.L., "Experimental study of influence of temperature of liquid on change in the rate of boiling", USAEC Report – AEC Trans. 3405, pp. 95-100, 1953.
- 4 Ivey, H.J. and Morris, D.J., "CHF of saturation and subcooled pool boiling in water at atmospheric pressure", *Proc. 3<sup>rd</sup> Int. Heat Transfer Conf.*, pp. 129, 1966.
- 5 Hwang, U. P. and Moran, K. P., "Boiling heat transfer of silicon integrated circuits chip mounted on a substrate", *Heat Transfer in Electronic Equipment*, ASME HTD- Vol. 20, pp. 53-59, 1981.
- 6 Morozov, V. G., "An experimental study of critical heat flux loads at boiling of organic liquids on a submerged heating surfaces", *Int. J. Heat Mass Transfer*, Vol. 2, pp. 252-258, 1960.
- 7 Lienhard, J.H. and Schrock, V.E. "The effect of pressure, geometry, and the equation of state upon the peak and minimum boiling heat flux", *J. Heat Transfer*, Vol. 85, pp. 261-272, 1963.
- 8 Lienhard, J.H. and Watanabe, K., "On correlating the peak and minimum boiling heat fluxes with pressure and heater configuration", *J. Heat Transfer*, Vol. 88, pp. 94-100, 1966.
- 9 Bergles, A.E. and Kim, C.J., "A method to reduce temperature overshoots in immersion cooling of microelectronics devices", *IEEE CH2590-8/88/0000-0100*, pp. 100-105, 1988.
- 10 Anderson, T. M., and Mudawar, I., "Microelectronic cooling by enhanced pool boiling of a dielectric fluorocarbon liquid," *Transactions of the ASME* Vol. 11, pp. 752-759, 1989.
- 11 Carvalho, R.D.M. and Bergles, A.E., "The influence of subcooling on the pool nucleate boiling and critical heat flux of simulated electronic chips", 1990 IHTC, pp. 289-294, 1990.
- 12 Bergles, A.E., "What is real mechanism of CHF in pool boiling", *Pool and External Flow Boiling ASME 1992*, pp. 165-170, 1992.
- 13 McNeil, A.C., "Pool boiling critical heat flux in a highly wetting liquid", *Master's Thesis*, University of Minnesota, Minneapolis, 1992.
- 14 Carvalho, R. D. M. and Bergles, A. E., "The effects of the heater thermal conductivity/capacitance on the pool boiling critical heat flux", *Pro. Engineering Foundation Conference on Pool and External Flow Boiling*, Santa Barbara, CA, pp. 203-212, 1992.
- 15 Brusstar, M. J. and Merte, "Effects of heater surface orientation on the critical heat Flux- II. A model for pool and forced convection subcooled boiling", *Int. J. Heat Mass Transfer*, Vol. 40, No. 17, pp. 4021-4031, 1997.
- 16 Bergles, A.E., "Enhancement of phase-change heat transfer", *Convective Flow and Pool Boiling*, pp. 23-31, 1998.
- 17 Lee, T.Y.T, Mahalingam, M., and Normington, P. J. C., "Subcooled pool Boiling Critical Heat Flux in dielectric liquid mixtures", 28<sup>th</sup> National Heat Transfer Conference, ASME HTD- Vol. 206, pp. 55-62, 1992.
- 18 Watwe, A. A., "Measurement and prediction of the pool boiling Critical Heat Flux in highly wetting liquids", Ph.D. Thesis, University of Minnesota, 1996.
- 19 Watwe, A. A. and Bar-Cohen, A., "Nucleate pool boiling and critical heat flux in gas-saturated dielectric coolants", 2<sup>nd</sup> European Thermal Sciences Conference and 14<sup>th</sup> UIT National Heat Transfer Conference, pp. 1631-1638, 1996.
- 20 Watwe, A.A., Bar-Cohen, A., and McNeil, A., "Combined pressure and subcooling effects on pool boiling from a PPGA chip package", *J. of Electronics Packaging*, pp. 95-105, June 1997.
- 21 Arik, M. and Bar-Cohen, A., "Immersion cooling of high heat flux microelectronics with dielectric liquids", 4<sup>th</sup> Int. Symposium and Exhibition on Advanced Packaging-Materials- Processes- Properties, Atlanta, pp. 229-247, 1998.



- 22 Kandlikar, S.G., "Critical heat flux in subcooled flow boiling- An assessment of current understanding and future directions for research", Boiling 2000- Engineering Science Foundation Conf., Alaska, 2000.
- 23 Arik, M., "Enhancement of pool boiling critical heat flux in dielectric liquids", Ph.D. Dissertation, Department of Mechanical Engineering, University of Minnesota, 2001.
- 24 Rainey, K.N., You, S.M., and S. Lee, "Effect of pressure, subcooling, and dissolved Gas on pool boiling heat transfer from microporous surfaces in FC-72", J. Heat Transfer, Vol. 125, No.1, pp. 75-83, 2003.
- 25 Arik, M. and Bar-Cohen, A, "Effusivity-based correlation of surface property effects in pool boiling CHF of dielectric liquids", Int. J. of Heat and Mass Transfer, Vol. 46, pp. 3755-3765, 2003.
- 26 El-Genk, M.S., and Parker, J.S., "Enhanced boiling of HFE-7100 dielectric liquid on porous graphite," Energy Conversion and Management, Vol. 46, pp. 2455-2481, 2005.
- 27 M. Arik, A. Kosar, H. Bostanci, A. Bar-Cohen, "Pool Boiling Critical Heat Flux in Dielectric Liquids and Nanofluids", Advances in Heat Transfer, Ed. Young Cho and George Greene, Vol. 43, 2011, pp. 1-76.
- 28 Arik, M., Bar-Cohen, A., and You, S.M., "Enhancement of pool boiling dielectric liquid critical heat flux by microporous coatings", Int. J. of Heat and Mass Transfer, Vol. 50, pp. 997-1009, 2007.
- 29 Arik, M. and Bar-Cohen, A, "Pool boiling of perfluorocarbon mixtures on silicon surfaces" International Journal of Heat and Mass Transfer, 2010.
- 30 Rohsenow, W.M., "Heat transfer with boiling", *Modern Developments in Heat Transfer*, The MIT Press, Cambridge, MA, pp. 169-260, 1964.
- 31 Incropera, Frank P., DeWitt, David P., "Introduction to Heat Transfer", Fifth Edition, John Wiley and Sons, 2006